Femtosecond Coincidence Imaging of Multichannel Multiphoton Dynamics

Anouk M. Rijs and Maurice H. M. Janssen
Laser Centre and Department of Chemistry, Vrije Universiteit, de Boelelaan 1083, 1081 HV Amsterdam, The Netherlands

Engelene t. H. Chrysostom and Carl C. Hayden
Combustion Research Facility, Sandia National Laboratories, P.O. Box 969, Livermore, California 94551-0969, USA
(Received 8 September 2003; published 26 March 2004)

The novel technique of femtosecond time-resolved photoelectron-photoion coincidence imaging is applied to unravel dissociative ionization processes in a polyatomic molecule. Femtosecond coincidence imaging of CF_3I photodynamics illustrates how competing multiphoton dissociation pathways can be distinguished, which would be impossible using photoelectron or ion imaging alone. Ion-electron energy correlations and photoelectron angular distributions reveal competing processes for the channel producing ($e^- + CF_3^+ + I$). The molecular-frame photoelectron angular distributions of the two major pathways are strikingly different.

DOI: 10.1103/PhysRevLett.92.123002 PACS numbers: 33.50.Hv, 33.60.Cv, 33.80.Eh, 33.80.Gj

Multiphoton excitation in molecular photodynamics enables studies of highly excited states and their complex decay dynamics. Intense femtosecond laser pulses easily induce multiphoton excitation and provide the time resolution needed to study the dynamics. Multiphoton excitation resulting in ionization frequently reveals multiple, complex ionization and fragmentation channels that are not seen in single-photon ionization. Compared to single-photon ionization, the multiphoton excitation accesses different Franck-Condon factors via resonant intermediate states and changes the probability of multielectron excitation processes. The energetics and vector correlations of dissociative ionization processes can be studied in complete detail using recently developed coincident imaging techniques [1]. Different energetically accessible dissociation channels can be identified from photoelectron-photoion energy correlations. Vector correlations, such as photoelectron angular distributions (PADs), provide information on the symmetry, electronic configuration, and orientation of the molecule as the electron is ejected [2–5]. So far, photoelectron-photoion coincident (PEPICO) imaging techniques have been mostly applied in ionization studies using one-photon excitation with synchrotron or He(I) radiation [6–11]. Only recently, first femtosecond time-resolved PEPICO imaging experiments were reported [12,13], and new theoretical frameworks have been developed to study time-resolved photoelectron dynamics [14,15]. In this Letter we use the full potential of time-resolved coincidence imaging to unravel competing ionization and fragmentation processes in multiphoton excited CF_3I.

The CF_3I molecule is investigated because it exhibits a variety of interesting dissociative ionization processes. It is one of the few polyatomic molecules for which these processes have been previously explored by both single and multiphoton excitation [6,7,16–18]. In particular, Powis and co-workers have used PEPICO imaging coupled with single-photon ionization sources [e.g. He(I)] to probe the dissociation of the $\tilde{A}^2A_1$ state of CF_3I^+ and measure molecular-frame PADs (MF-PADs) associated with the CF_3^+ and I^+ fragments [6]. Here we apply femtosecond time-resolved multiphoton excitation of CF_3I to the region just below the $\tilde{A}^2A_1$ state of CF_3I^+ and follow the production of $CF_3^+ + I$ fragments using the PEPICO imaging apparatus at Sandia National Laboratories [1,12,13].

In the experiments, a regeneratively amplified Ti:sapphire laser operating at 0.7 kHz produces linearly polarized laser pulses at 795 nm. The compressor output, with typical pulse duration of about 100 fs, is frequency doubled and tripled. The pump pulse (centered at 265 nm, pulse energy $\sim$13 μJ) and the probe pulse (centered at 398 nm, pulse energy $\sim$11 μJ) are focused (focal length 1 m) into an ultrahigh vacuum chamber where they intersect the pulsed molecular beam (6% CF_3I in argon). The electrons and ions, detected in coincidence, are accelerated in opposite directions towards time- and position-sensitive detectors [12]. From the arrival time and position the initial velocity vector is calculated for each detected fragment and its associated electron.

Figure 1 shows a schematic of the energy levels of CF_3I relevant to this experiment. CF_3I is excited with two pump photons at 265 nm to an energy region where a short lived $7s\sigma$ Rydberg state has been identified [19]. The excitation is also resonant at the one-photon level with the very short lived dissociative neutral A band. This one-photon resonance has prevented detailed spectroscopic resonance-enhanced multiphoton ionization studies with nanosecond lasers in the energy region of the $7s\sigma$ Rydberg state. In contrast, the lower energy region in the $6s$-$6p$ Rydberg states has been extensively studied with nanosecond lasers [20,21]. In our experiments, a time delayed probe pulse at 398 nm ionizes CF_3I at a total energy of 12.48 eV, which accesses several ionization

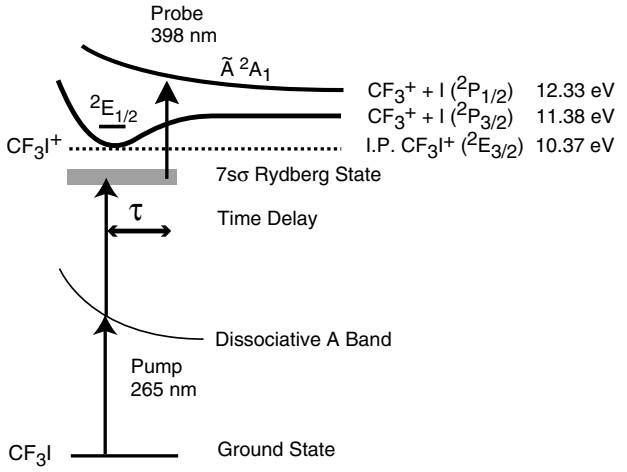

FIG. 1. Energy level scheme of the most relevant states of CF_3I, using the energies from Refs. [18,19]. The total $(2 + 1')$ photon excitation is at 12.48 eV.

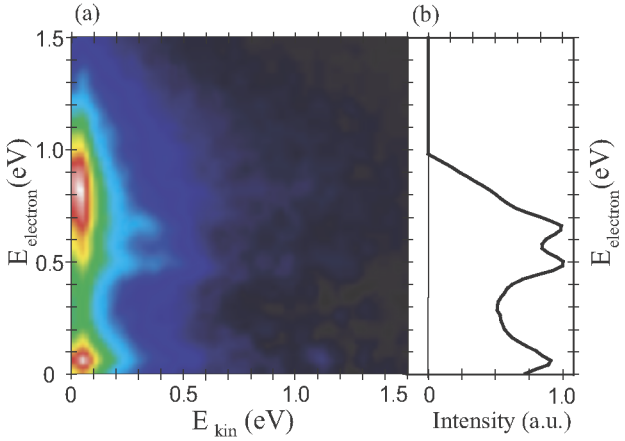

FIG. 2 (color online). (a) Photoelectron-photoion energy correlation spectrum of (e^-, CF_3^+) at 300 fs time delay. (b) The electron spectrum for events with CF_3^+ ions within a range of total center-of-mass kinetic energy of $0.25 \leq E_{kin} \leq 0.50$ eV, and total energy less than 1.2 eV.

limits, the CF_3I^+ ($\tilde{X}\,^2E_{3/2}$) ionic ground state at 10.37 eV, the spin-orbit excited $\tilde{X}\,^2E_{1/2}$ state at 11.10 eV, the lowest ionic dissociation channel at 11.38 eV producing $CF_3^+ + I(^2P_{3/2})$ [18], and the $CF_3^+ + I(^2P_{1/2})$ dissociation threshold. Absorption of a second probe photon is also observed resulting in fragmentation to the other ionic channel $CF_3 + I^+$. At the time delay reported here (~300 fs) ionization yielding fragment ions, CF_3^+ or I^+ dominates strongly over ionization to the parent CF_3I^+ [16,17], which suggests that ionization occurs from a vibrationally excited neutral molecule. The coincidence data allow us to select from all the measured (e^-, ion) coincidence events those corresponding to a particular ion mass. In this Letter we discuss only the channel producing ($e^- + CF_3^+ + I$).

Figure 2 presents an energy correlation spectrum for the dissociative ionization that yields CF_3^+. The total number of (e^-, CF_3^+) events in this data set is ~435 000. A background contribution from the 265 nm pump alone is carefully substracted to plot the data in Fig. 2. In the energy correlation spectrum the joint probability distribution of the center-of-mass fragment recoil energy (along the x axis) and the coincident photoelectron kinetic energy (along the y axis) are plotted for all (e^-, CF_3^+) events. The center-of-mass fragment translational energy is the sum of the measured CF_3^+ ion recoil and the corresponding I atom recoil, determined from conservation of linear momentum. Figure 2 clearly shows that multiple ionization processes produce CF_3^+. Since energy conservation limits for the $(2 + 1')$ scheme ($E_{max} \approx 1.2$ eV including effects of instrumental resolution) are not violated, the CF_3^+ photofragments are the result of one probe photon ionization. Upon increasing the probe laser intensity substantially we did observe in the energy correlation spectrum additional (e^-, CF_3^+) ionization events from the absorption of two probe photons. In the lower left corner of the correlation spectrum there is a peak corresponding to slowly recoiling CF_3^+ ions in coincidence with low energy electrons. This peak results from near threshold ionization to the barely accessible $CF_3^+ + I(^2P_{1/2})$ dissociation asymptote. This process will not be considered further in this Letter. Another ionization process results in slowly recoiling CF_3^+ photofragments formed in coincidence with electrons that are ejected with high energies, around 0.85 eV. The third ionization pathway produces CF_3^+ ionic fragments with a range of recoil velocities (E_{kin} up to ~0.50 eV) coincident with electrons, which have discrete photoelectron kinetic energies. This process is identified in the energy correlation plot by the horizontal stripes at electron energies of ~0.5 and ~0.7 eV. A vertical slice through the energy correlation plot gives the photoelectron kinetic energy distributions for the selected (e^-, CF_3^+) events. In Fig. 2(b) the photoelectron spectrum of events with fragment center-of-mass kinetic energies of $0.25 \leq E_{kin} \leq 0.50$ eV is displayed. A clear structure with peaks separated by ~0.2 eV is observed which is not apparent in the complete photoelectron spectrum.

To further distinguish the two different ionization pathways that produce higher energy electrons we extract PADs in both the laboratory frame (LF-PAD) and the molecular frame (MF-PAD). The former is obtained by determining the angle of the electron recoil vector with respect to the polarization axes of the pump and probe lasers (parallel in our case). The latter is obtained by calculating the angle between the fragment ion recoil vector and the coincident electron recoil vector. The MF-PAD reflects the electron recoil angular distribution relative to the molecular symmetry axis assuming the ionization or dissociation is axial and fast [1]. The

MF-PADs are plotted for selected photoelectron-photoion events with the CF_3^+ fragments recoiling nearly along the laser polarization axis (±15°) so the resulting 3D MF-PADs are azimuthally isotropic about the dissociation axis.

In Fig. 3, the LF-PADs and MF-PADs are shown for the two energy windows described above at 300 fs time delay. The LF-PADs [Figs. 3(a) and 3(d)] are necessarily symmetric about $\cos(\theta_{LF}) = 0$, because the orientation of the CF_3I molecule is not selected. The LF-PADs show only a small difference, suggesting that ionization may result from different electronic transitions. In contrast, the MF-PADs for the two energy regions are strikingly different, indicating that two completely different dissociative ionization processes are occurring. The MF-PAD for the slowly recoiling CF_3^+ photofragments associated with 0.8 to 1.2 eV electrons [Figs. 3(b) and 3(c)] is forward-backward symmetric. The electrons are ejected preferentially along the dissociation axis but with equal probability toward and away from the recoiling CF_3^+. Surprisingly, the MF-PAD for the CF_3^+ fragments associated with the region of discrete electron energies at 0.5 and 0.7 eV [Figs. 3(e) and 3(f)] is strongly forward-backward asymmetric, the electrons are preferentially recoiling in the direction of the CF_3^+ ionic fragment. To produce this strong asymmetry, the dissociation must be fast compared to the molecular rotation time, but some smearing of the MF-PAD due to rotation cannot be ruled out [7,8]. The shape of the MF-PAD is nearly constant through the 0–0.5 eV recoil energy range observed for CF_3^+ fragments, so events within this entire range were used to generate the MF-PADs displayed in Fig. 3. The azimuthally isotropic PADs are fitted to a linear expansion of Legendre polynomials, $P_i(\cos\theta_{MF})$, up to the fourth order, $N = 4$ [2]:

$$I(\theta_{MF}) = \frac{\sigma}{4\pi}\left[1 + \sum_{i=1}^{N} \beta_{i,MF} P_i(cos\theta_{MF})\right], \qquad (1)$$

where θ_{MF} is the angle between the recoil direction of the ion and the ejected electron and β_i fit parameters. We find that for the fast electron channel $\beta_{1,MF} \approx 0.0$, whereas for the channel with discrete electron energies $\beta_{1,MF} \approx 0.52$, i.e., a very oriented MF distribution.

The slowly recoiling CF_3^+ photofragments associated with 0.8 to 1.2 eV electrons result from the direct ionization of excited neutral molecules to vibrationally excited CF_3I^+ ions. The vibrationally excited parent ions undergo rapid unimolecular dissociation to $CF_3^+ + I$. The angular distribution of the recoiling CF_3^+ fragments (not shown here) is peaked along the laser polarization axis, indicating that the dissociation is relatively rapid. The MF-PAD shows no correlation between the electron recoil direction and the orientation of the dissociation axis, implying that the ionization and dissociation process are not closely coupled.

The ionization process that produces the horizontal stripe features in the energy correlation spectrum is unusual in that no correlation between the electron and fragmentation energies is observed, while a strong angular correlation between the electron recoil direction and the molecular dissociation axis is seen in the MF-PADs. If this were a direct dissociative ionization, an inverse relationship between the electron and photofragment recoil energies would be expected [1,12]. For example, higher fragment recoil energies would correlate with lower electron energies.

One possibility for the origin of the horizontal features in the energy correlation spectrum is the ionization of electronically excited neutral CF_3 from photofragmentation of neutral CF_3I. This is difficult to completely rule out due to the lack of knowledge about the excited electronic states of CF_3. However, we would expect an excited neutral CF_3 Rydberg state photofragmentation product to

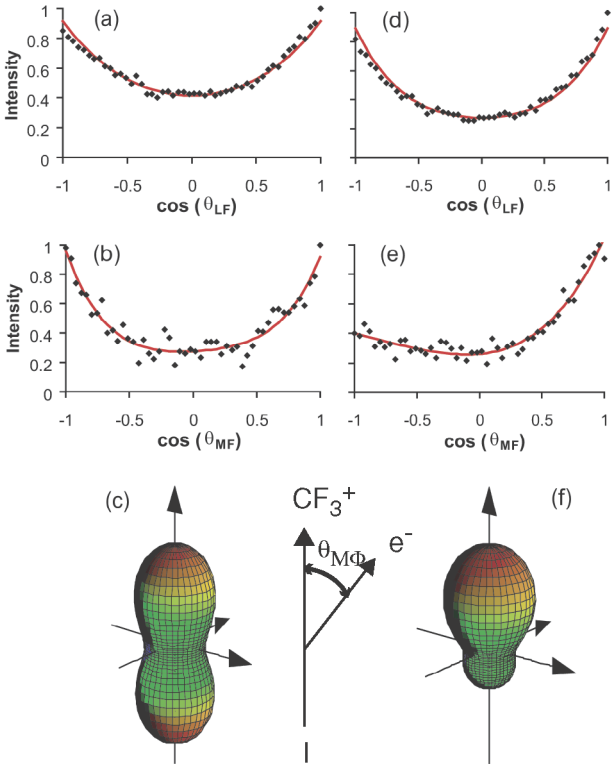

FIG. 3 (color online). (a) Experimental LF-PAD, at 300 fs delay, of electrons within the energy range 0.80–1.17 eV and CF_3^+ ions with total kinetic energy 0–0.18 eV. (b) Experimental MF-PAD for (e^-, CF_3^+) events with energies as in (a). (c) A 3D representation of the fitted Legendre representation of the MF-PAD of the experimental data of (b). (d) Experimental LF-PAD, at 300 fs delay, of electrons within the energy range 0.38–0.78 eV and CF_3^+ ions with total kinetic energy 0.0–0.50 eV. (e) Experimental MF-PAD (e^-, CF_3^+) events with energies as in (d). (f) A 3D representation of the fitted Legendre representation of the MF-PAD of the experimental data of (e).

be planar and thus not show forward-backward asymmetry in its MF-PAD.

Instead, we assign the region containing the horizontal stripes in the energy correlation spectrum to electronic autoionization. The autoionizing state is probably in a Rydberg series converging to the dissociative $\tilde{A}^2A_1$ ionic limit. The excited dissociative ionic $\tilde{A}^2A_1$ state has a vertical ionization energy of 12.75 eV [18]. In our experiments for $(2 + 1')$ ionization the total photon energy is 12.48 eV, which is only $\sim$0.27 eV below the electronically excited ionic $\tilde{A}$ state. Here a plethora of superexcited states belonging to series converging upon the $\tilde{A}$ state can be expected. In fact, Asher and Ruscic [22] observed a strong and broad autoionizing feature extending into this region. Since the $\tilde{A}^2A_1$ state is dissociative, the autoionizing state is also likely dissociative. Thus, upon excitation the CF_3I molecule starts to dissociate on the potential of this superexcited state. The ionization must occur before the CF_3I completely dissociates because the presence of the iodine is necessary to break the forward-backward symmetry along the dissociation axis and produce the resulting asymmetric MF-PAD. The electron peak around 0.7 eV corresponds with the energy difference between the spin-orbit states of the CF_3I^+ ground state of 0.73 eV (see Fig. 1). The electronic autoionization may therefore be spin-orbit induced, ejecting electrons with energy close to the spin-orbit splitting. The peak at 0.5 eV is shifted by an amount close to the energy of the CF stretch of the $CF_3{}^+$ ion ($\approx$0.2 eV). Thus autoionization populates at least two C-F stretching vibrational states in the dissociating CF_3I^+. Note that the $CF_3{}^+$ fragment is planar and has a higher frequency C-F stretch than the pyramidal CF_3I^+ parent ion so these structural changes will induce vibrational excitation.

In these experiments using femtosecond ionization through an intermediate in the region of the 7*s* Rydberg state we observe multiple dissociative ionization channels with a strong autoionization process. This differs from results of ionization through the 6*p* Rydberg state using nanosecond lasers. There, only direct ionization to the ground state of CF_3I^+ is observed and photofragmentation of this ion produces $CF_3{}^+$ fragments [18]. The correlated energetic and angular data available from femtosecond PEPICO imaging experiments have proven essential for identifying the multiple dissociative ionization processes observed. The energy correlation spectra show features that are not apparent in either the photoelectron or the ion recoil spectra alone, and the MF-PADs are unavailable without the measurement of correlated electron and fragment recoil velocity vectors.

The authors thank M. Gutzler for expert technical assistance and Dr. S. T. Pratt and Professor C. A. de Lange for helpful discussions. A. M. R. acknowledges the Holland Research School of Molecular Chemistry for support and the council for Chemical Sciences of the Netherlands Organization for Scientific Research (CW-NWO) for travel support. A. M. R. and M. H. M. J. thank the CRF/Sandia National Laboratory Visitors program for financial support. The research of E. t. H. C. and C. C. H. is supported by Division of Chemical Sciences, Geosciences and Biosciences, the Office of Basic Energy Sciences, the U.S. Department of Energy. Sandia is a multiprogram laboratory operated by Sandia Corporation, a Lockheed Martin Company, for the United States Department of Energy's National Nuclear Security Administration under Contract No. DE-AC04-94AL85000.

[1] R. E. Continetti and C. C. Hayden, *Advanced Series in Physical Chemistry: Modern Trends in Chemical Reaction Dynamics* (World Scientific Publishing, Singapore, 2004).
[2] N. Chandra, J. Phys. B **20**, 3405 (1987).
[3] N. Watanabe, J. Adachi, K. Soejima, E. Shigemasa, and A. Yagishita, Phys. Rev. Lett. **78**, 4910 (1997).
[4] Y. Hikosaka, J. Eland, T. Watson, and I. Powis, J. Chem. Phys. **115**, 4593 (2001).
[5] T. Seideman, Annu. Rev. Phys. Chem. **53**, 41 (2002).
[6] P. Downie and I. Powis, Phys. Rev. Lett. **82**, 2864 (1999).
[7] P. Downie and I. Powis, J. Chem. Phys. **111**, 4535 (1999).
[8] P. Downie and I. Powis, Faraday Discuss. **115**, 103 (2000).
[9] A. V. Golovin, F. Heiser, C. J. K. Quayle, P. Morin, M. Simon, O. Gessner, P.-M. Guyon, and U. Becker, Phys. Rev. Lett. **79**, 4554 (1997).
[10] A. Lafosse, M. Lebech, J. Brenot, P. Guyon, O. Jagutzki, L. Spielberger, M. Vervloet, J. Houver, and D. Dowek, Phys. Rev. Lett. **84**, 5987 (2000).
[11] T. Osipov, C. Cocke, M. Prior, A. Landers, T. Weber, O. Jagutzki, L. Schmidt, H. Schmidt-Böcking, and R. Dörner, Phys. Rev. Lett. **90**, 233002 (2003).
[12] J. A. Davies, J. E. LeClaire, R. E. Continetti, and C. Hayden, J. Chem. Phys. **111**, 1 (1999).
[13] J. A. Davies, R. E. Continetti, D.W.Chandler, and C. Hayden, Phys. Rev. Lett. **84**, 5983 (2000).
[14] Y. Arasaki, K. Takatsuka, K. Wang, and V. McKoy, J. Chem. Phys. **114**, 7941 (2001).
[15] Y. Suzuki, M. Stener, and T. Seideman, Phys. Rev. Lett. **89**, 233002 (2002).
[16] W. G. Roeterdink and M. H. M. Janssen, Chem. Phys. Lett. **345**, 72 (2001).
[17] W. G. Roeterdink and M. H. M. Janssen, Phys. Chem. Chem. Phys. **4**, 601 (2002).
[18] F. Aguirre and S. T. Pratt, J. Chem. Phys. **118**, 6318 (2003).
[19] L. H. Sutcliffe and A. D. Walsh, Trans. Faraday Soc. **57**, 873 (1961).
[20] C. A. Taatjes, J.W. G. Mastenbroek, G. v. d. Hoek, J. G. Snijders, and S. Stolte, J. Chem. Phys. **98**, 4355 (1993).
[21] N. A. Macleod, S. Wang, J. Hennessy, T. Ridley, K. P. Lawley, and R. J. Donovan, J. Chem. Soc., Faraday Trans. **94**, 2689 (1998).
[22] R. Asher and B. Ruscic, J. Chem. Phys. **106**, 210 (1997).